N91-23005



## GEOLOGY, STRUCTURE, AND STATISTICS OF MULTI-RING BASINS ON MARS.

*Richard A. Schultz and Herbert V. Frey, NASA Goddard Space Flight Center, Greenbelt, MD 20771.*

Multi-ring basins define the fundamental tectonic framework upon which subsequent geologic and geophysical processes of many planets and satellites are superimposed. For example, most volcanic and tectonic activity on the Moon was localized by pre-existing impact basins [1]. Control of volcanism, tectonics, erosion, and perhaps even volatile dynamics on Mars by multi-ring basins can be discerned in many areas [2] even though endogenic processes were quite vigorous over the planet's history. On the other hand, the family of impacting objects that produced these basins is probably related to planetary accretion [3], and size-frequency characteristics of impactor populations can be estimated given an accurate inventory of impact craters and basins [4]. Thus the record of multi-ring basins on Mars provides a fundamental link between the planet's accretion and its later development.

We have compiled and evaluated available data on martian multi-ring basins [5] using the new 1:15 milion scale geologic maps of Mars [6] and revised global topography [7] as base maps. Published center coordinates and ring diameters of martian basins were plotted by computer and superimposed onto the base maps. In many cases we had to adjust basin centers or ring diameters or both to achieve a better fit to the revised maps. We also found that additional basins can explain subcircular topographic lows as well as map patterns of old Noachian materials, volcanic plains units, and channels in the Tharsis region [8].

Smaller impact basins on Mars such as Ladon (D = 975 km) are comparable dimensionally, morphologically, and structurally to Orientale (D = 930 km) on the Moon. In contrast, Orientale-type morphology can be recognized only for martian basins smaller than Argyre (D = 1850 km). Larger basins such as Isidis, Argyre, and Hellas typically show a rugged, blocky annulus with concentric grabens surrounding a central depression. Still larger structures show either multiple rings reminiscent of Valhalla on Callisto (Chryse) or persistent depressions surrounded by poorly expressed concentric structure (Elysium [9], Utopia [10]). Basin relief relative to diameter becomes progressively shallower with increasing basin diameter. Thus, the morphology and structure of martian multi-ring basins changes significantly as basins increase in size.

The formation of concentric ring structure and post-impact viscous relaxation of basin topography can differ for spherical, rather than planar, targets [11,12]. Diameters of martian multi-ring basins can be significant fractions of Mars' radius. For example, ratios of basin diameter to planetary radius are: Elysium, 1.46; Utopia, 1.39; Chryse, 1.06; Hellas, 0.68; Argyre, 0.55; and Ladon, 0.29. The value for Argyre is comparable to that of Orientale normalized by lunar radius, 0.53, or Caloris on Mercury, 0.53. Because Argyre, Orientale, and Caloris have similar normalized diameters but different morphologies, planetary curvature by itself probably did not control the morphology of these moderate sized basins. Structures larger than Chryse may have been influenced by spherical target geometry.

R-plots of basin diameters (Fig. 1) show that the martian multi-ring basin population dovetails into the smaller crater population [13] near 500 km diameter. The relative abundance of basins >1000 km in diameter is comparable on Mars and the Moon, perhaps suggesting an inner solar system source for the larger impactors [e.g., [4]). R-plots and weighted least squares fit to cumulative frequency data (Fig. 2) both indicate that basins follow a shallow production function. Basins 500 to 1500 km in diameter show the characteristic Orientale morphology and a best-fit slope of $D^{-0.75}$. Basins larger than Argyre define a $D^{-1.7}$ slope. The slope change may in part reflect the size-frequency population of the largest impactors. Formation of large multi-ring basins on early Mars may be more analogous mechanically to impacts on icy satellites (e.g., [14,11]) than to late forming lunar basins. Thus, Orientale morphology may not scale linearly to the largest diameters on Mars.

**REFERENCES:** [1] Solomon & Head (1980) *Rev. Geophys., 18*, 107-141. [2] Schultz, Schultz, & Rogers (1982) *JGR, 87*, 9803-9820. [3] Wetherill (1977) *Proc. Lunar Sci. Conf., 8th*, 1-16; Wetherill (1981) in Multi-ring Basins, *Proc. Lunar Planet. Sci. 12A*, 1-18. [4] Strom (1987) *Icarus, 70*, 517-535. [5] R. Schultz & Frey (1989) *JGR*, submitted. [6] Scott & Tanaka (1986) USGS *Map I- 1802-A*; Greeley & Guest (1987) USGS *Map I-1802-B*; Tanaka & Scott (1987) USGS *Map I-1802-C*. [7] Wu et al. (1986) PGPI-1985, NASA TM-88383, 614-617. [8] Frey & Schultz (1989) 4th Mars Conf., 106-107. [9] P. Schultz (1984) Lunar Planet. Sci., XV, 728-729. [10] McGill (1989) *JGR, 94*, 2753-2759. [11] Melosh (1982) *JGR, 87*, 1880-1890. [12] Thomas & Squyres (1988) *JGR, 93*, 14,919-14,932. [13] Barlow (1988) *Icarus, 75*, 285-305. [14] McKinnon & Melosh (1980) *Icarus, 44*, 454- 471.

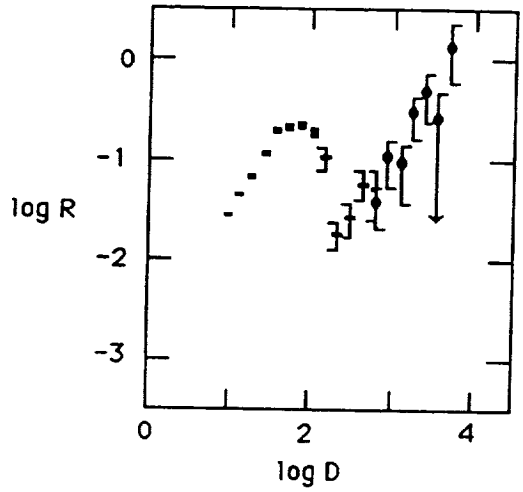


*Fig. 1. Relative frequency (R-plot) diagrams of martian craters and basins. Data for basins < 500 km in diameter from Barlow [1988].*

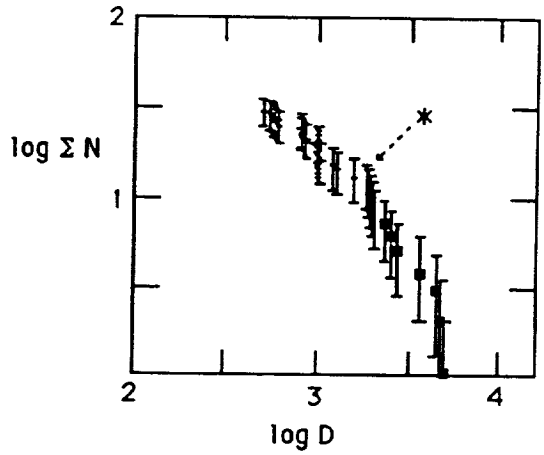


*Fig. 2. Cumulative frequency distribution of martian multi-ring basins > 500 km in diameter (unbinned data). Data normalized by surface area of Mars. Basins > 2300 km in diameter shown by dots; Argyre shown by *.*

EVIDENCE FOR MULTIPLE FLOODING EPISODES IN KASEI VALLES, MARS;
D.H. Scott and James M. Dohm, U.S. Geological Survey, Flagstaff, AZ 86001.

Kasei Valles make up one of the largest systems of outflow channels on Mars. They were a major contributor of water into the Chryse basin during the Late Hesperian and possibly Early Amazonian Epochs. The walls and floors of the valleys are terraced and grooved, closely resembling the Channeled Scablands of eastern Washington State that were formed by catastrophic floods probably lasting no more than a few days [1,2]. Previous geologic mapping [3] of parts of Kasei Valles was not conclusive as to whether water levels varied markedly during a single flood and erosional event or whether flooding was episodic and marked by intermittent periods of scouring. This problem--whether one or several flood episodes occurred within individual water courses--has been a continuing issue in studies of Martian channel formation [4]. Recent large-scale geologic mapping [5] of Mangala Valles, another large outflow channel system in the Memnonia region of Mars, shows deposits of two periods of flooding, which are separated stratigraphically by an intervening lava flow. In other areas around the Chryse basin, geologic studies, e.g., [4] have indicated that more than one episode of channel formation occurred or, less likely, that flooding was of very long duration.

Our present mapping of flood-deposited materials in Kasei Valles on high-resolution photomosaic bases (1:500,000 scale) shows cross-cutting flow and scour lines along water courses that may indicate separate flood events (Fig. 1); more definitively, morphologies of craters clearly distinguish them as having formed before, between, and after separate flood stages (Figs. 2-3). Counts of craters (≥2-km rim-crest diameter) made on smooth and grooved parts of the Kasei floor also indicate floods of at least two different ages: $253\pm96/10^6$ km$^2$ (Early Amazonian) and $910\pm148/10^6$ km$^2$ (intermediate Hesperian); previous crater counts in Kasei Valles [6,7], though less directed toward specific events, generally confirm our results.

REFERENCES

[1] Baker, V.R. and D.J. Milton (1974) Icarus 23, 27-41.
[2] Baker, V.R. and R.C. Kochel (1979) Jour. Geophys. Res. 84, 7961-7983.
[3] Chapman, M.G. and D.H. Scott (1989) Proc. 19th Lunar and Planet. Sci. Conf., 367-375.
[4] Greeley, R., E. Theilig, J.E. Guest, M.H. Carr, Harold Masursky, and J.A. Cutts (1977) Jour. Geophys. Res. 82, 4093-4109.
[5] Tanaka, K. and Chapman, M.G. (1990) Jour. Geophys. Res., in press.
[6] Carr, M.H. and G.D. Clow (1981) Icarus 48, 91-117.
[7] Neukum, G. and K. Hiller (1981) Jour. Geophys. Res. 86, 3097-3121.

KASEI VALLES REGION FLOOD FEATURES

Figure 1. Scoured and grooved channel floor; arrows show three directions of water flow possibly indicative of separate flood events (Viking image 226A10, centered near lat 25° N., long 61°).

Figure 2. Impact crater in channel; crater was formed before and degraded by early catastrophic flooding that scoured channel floor (Viking image 664A07, centered near lat 23° N., long 74°).

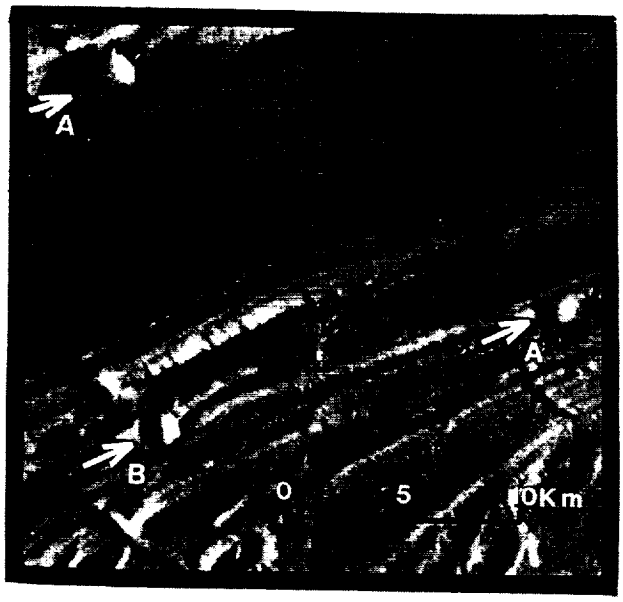


Figure 3. Impact craters (arrows at A) formed after early high-water stage that deeply eroded terraces; craters have been truncated by later floods along lower part of valley floor. A post-flood crater is shown at B (Viking image 665A20, centered near lat 27° N., long 68°).

MOTTLED TERRAIN: A CONTINUING MARTIAN ENIGMA; D.H. Scott and J.R. Underwood, (1) U.S. Geological Survey, Flagstaff, Ariz. and (2) Kansas State University, Manhattan, Kansas

The northern lowlands of Mars are largely covered by plains materials that overall are mottled light and dark, a characteristic that is apparent on both Mariner and Viking images. The mottled terrain material (1) that makes up most of the northern lowlands is probably the most ambiguous material on all Martian images (2). Early studies, e.g., (3), used Mariner 9 images, which showed a hummocky, mottled surface encircling the planet between about lat 50° and 70° N. The Mariner pictures were degraded in this zone by atmospheric haze and high sun angles, which blurred them and produced high albedo contrasts; because significant morphologic variations were not recognized, the entire region was mapped as mottled plains material, a single geologic unit. Although image quality was poor, the mottling of the plains could be seen to result from albedo contrasts between numerous bright crater-ejecta blankets and dark intercrater plains material; also contributing to this effect were many dark-crested knobs, some having long, narrow, bright windstreaks or summit craters with bright interiors. The mottled plains were variously interpreted to consist of lava flows and knobby remnants of the highlands to the south (3), eolian and volcanic materials (4,5,6), ancient terrain and pedestal craters exhumed by wind erosion (7), eolian material cemented by permafrost (8), or volatile-rich deposits (9).

Debris mantles, suggested by (1) to have been derived from polar deposits, are distributed more or less symmetrically around the poles, extending as far as 30° toward the equator. These authors further suggested that the northern hemispheric mantle blankets the mottled plains and masks small (≤10-km diameter) craters on both young and old terrains.

I have described several geologic problems in the Martian northern plains, including that of the origin of the mottled material (2); I suggested that the plains "... may be an eroded remnant of the highlands that have survived a tectonic period of crustal separation caused by drifting or downfaulting followed by erosion."

The presence of lobate debris aprons, concentric crater fill, and terrain-softening poleward of lat 30° N. and S. suggested to (10) that topography in these regions has relaxed through quasi-viscous flow in ice-rich surface and near-surface materials. Support for this idea was provided by theoretical studies (11), which showed that ground ice should be present on Mars at middle and high latitudes. Dial (12) thought that permafrost and highly altered volcanic materials form the mottled plains.

Recent global geologic mapping of Mars (13,14,15), using high-resolution and high-quality Viking images, has subdivided the mottled terrain as originally mapped (3) into four members that constitute the Vastitas Borealis Formation of Late Hesperian age. The members intergrade and are largely distinguished by secondary morphologic characteristics, such as pronounced albedo contrasts, whorled patterns of ridges, knobby hills, and irregular troughs having polygonal outlines in places. Although the formation has been postulated to consist of lava flows, fluvial

deposits, and eolian materials within a permafrost zone (13), its surface is highly degraded, and the composition and origin of its component members remain uncertain.

Mapping problems still exist where image quality and resolution are adequate to determine textural characteristics of individual units but do not reveal the nature of their boundaries, stratigraphic relations, modes of formation, and processes responsible for their characteristic morphologies. The mottled plains material, as originally mapped and recently subdivided into members of the Vastitas Borealis Formation, continues to remain the most enigmatic geologic material in the northern hemisphere of Mars. Clarification of the origin of the mottled plains is critical, because this large, low, comparatively flat and unobstructed region may well provide the most suitable locations for successful landing and sample-return missions on Mars.

REFERENCES

(1) Soderblom, L. A., J. J. Kreidler, and H. Masursky (1973) J. Geophys. Res., 78, 4117-4122.
(2) Scott, D. H. (1979) Proc. Lunar Planet. Sci. Conf. 10, 3039-3054.
(3) Scott, D. H., and M. H. Carr (1978) U.S. Geol. Surv. Misc. Inv. Ser. Map I-1083.
(4) Greeley, R., and J. E. Guest (1978) U.S. Geol. Surv. Misc. Inv. Ser. Map I-1038.
(5) Lucchitta, B. K. (1978) U.S. Geol. Surv. Misc. Inv. Ser. Map I-1065.
(6) Morris, E. C., and K. A. Howard (1981) U.S. Geol. Surv. Misc. Inv. Ser. Map I-1286.
(7) Underwood, J. R., Jr., and N. J. Trask (1978) U.S. Geol. Surv. Misc. Inv. Ser. Map I-1048.
(8) Elston, W. E. (1979) U.S. Geol. Surv. Misc. Inv. Ser. Map I-1140.
(9) Wise, D. U. (1979) U.S. Geol. Surv. Misc. Inv. Ser. Map I-1154.
(10) Squyres, S. W., and M. H. Carr (1986) Science, 231, 249-252.
(11) Fanale, F. P., J. R. Salvail, A. P. Zent, and S. E. Postawko (1986) Icarus, 67, 1-18.
(12) Dial, A. (1984) U.S. Geol. Surv. Misc. Inv. Ser. Map I-1640.
(13) Scott, D. H., and K. L. Tanaka (1986) U.S. Geol. Surv. Misc. Inv. Ser. Map I-1802-A.
(14) Greeley, R., and J. E. Guest (1987) U.S. Geol. Surv. Misc. Inv. Ser. Map I-1802-B.
(15) Tanaka, K. L., and D. H. Scott (1987) U.S. Geol. Surv. Misc. Inv. Ser. Map I-1802-C.

THE RELATION OF THE LAVA COMPLEXES OF THE OLYMPUS MONS ON MARS. I.V. Shalimov, Moscow State University, Moscow, USSR.

The geological map of western equatorial region of Mars by David H.Scott and Kanneth L.Tannaka[I]shows the older ade of the shield lava complex of the Olympus Mons then the plain one. This conclusion is based on the crater density analysis. The detailed geolodical mapping gives us the possibility to obtain the contrary interpretation.

On the northeastern periphery of the shield complex one can observe the plain lava complex, partialy flooding the broken relief of the Olympus Mons aureole. Lavas from the shield complex overly the plain one and flood completely the broken relief of aureole(fig.2[2]). In the southeast one can observe lavas from the plain complex, flooding the Olympus Mons scarp. Lavas from the shield complex flow down from the scarp and form the flows on the surface of the plain complex(fig.3 [3]). In the southwest one can observe the shield lava complex overlying the plain one. In this case plain lavas flooding the depressions of the Olympus Mons aureole relief are isolated from their main area(fig.4[4]).

In addition along the all contact line one can observe the identity of lava flow directions in two complexes. It is known on the orientation of lava flow lobes. If the shield complex is older one should observe another ratio.

This consideration leads to the conclusion that the crater date analysis can give some incorrect results if it is applied to the small surface area. In this case it is necessary to preper the visual investigations and the detailed mapping been more objective analysis.

REFERENCES:
I.D.Scott and K.Tannaka Geology, western equatorial region of Mars. U.S. Geol. Surv. I986 I:I5000000, mapI-I802-A.
2.Atlas of Mars, topografic series, I:2000000: Tharsis northwest, M 2M 22/I24 CM I985,I-I62I /MC-9NW:revised/.
3.Atlas ofMars, ibid; Tharsis southwest, M 2M 7/I24 CM I985, I-I622 /MC-9SW:revised/.
4.Atlas of Mars, ibid;Amasonis southeast, M 2M 7/I46 CM I98I, I-I33I /MC-8SE/.

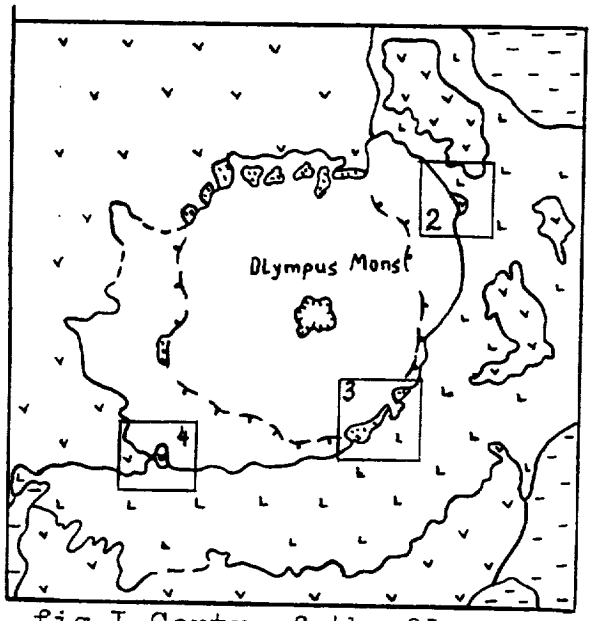


fig.I Centr of the Olympus Mons. The places of fig.2,3,4.

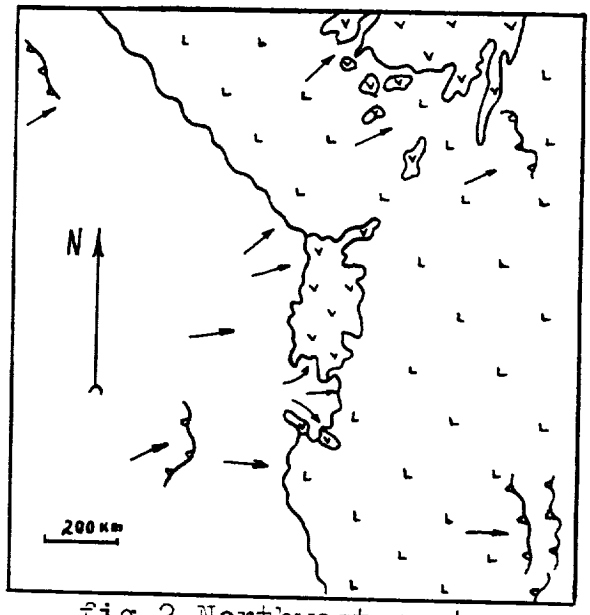


fig.2 Northwest part.

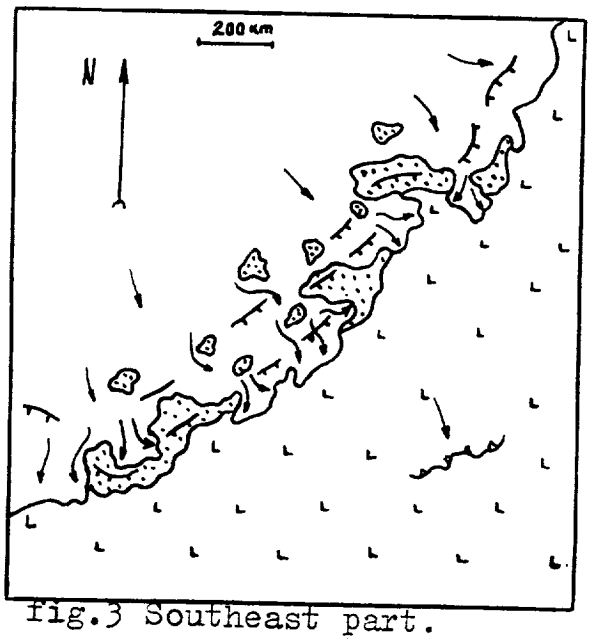


fig.3 Southeast part.

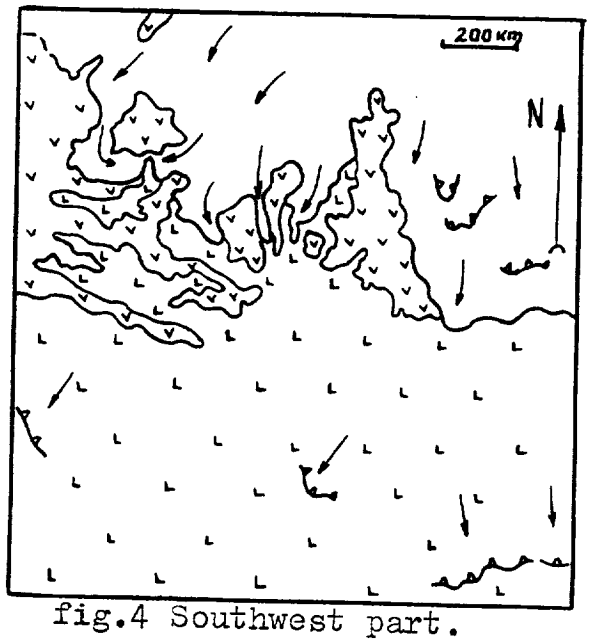


fig.4 Southwest part.


I-shield complex, 2-plains complex, 3-aureole complexes, 4-socle of Olympus Mons, 5-otherwise rocks, 6-direction of flow, 7-lobe of lava flow, 8-scarp of Olympus Mons, 9-caldera.

## VISIBLE AND NEAR-IR SPECTRAL IMAGING OF MARS DURING THE 1988 OPPOSITION.

Robert B. Singer, Jeffrey S. Miller, Kent W. Wells, and Ellen S. Bus, *Planetary Image Research Laboratory, Planetary Sciences Dept., University of Arizona, Tucson AZ 85721*

We conducted a major program of spectral imaging of Mars in the visible and near-IR (0.44-1.05$\mu$m) centered around the excellent 1988 opposition. The objective was to produce detailed reflectance spectra for contiguous, spatially resolved surface elements covering most of the planet. In this abstract we present some initial results from these observations.

A total of 6 observing runs, of 3-4 days duration each, were conducted on the University of Arizona's 1.5m telescope on Mt. Bigelow. Nearly all of Mars south of 40°N was observed at least once. Instrumentation consisted of the LPL Echelle Spectrograph (D. Hunten) and the LPL CCD system (U. Fink). A prism in the spectrograph gave spectral resolution of 2nm in the blue and 10nm in the near-IR. The best-case spatial resolution is 250km by 150km per pixel. Careful standard star observations were made to facilitate accurate spectrophotometric calibrations. Differential refraction in the Earth's atmosphere was also properly accommodated for. A photographic record of the slit position on Mars was made for every CCD exposure to allow the locations of our observations to be calculated accurately. These spectral images will eventually be calibrated to radiance factor ($R_F$) [1] through the solar analog star 16 Cyg B. The data presented here are calibrated in a relative sense to solar analog star HD1835: the zero reflectance level is accurately known, and the relative signal level from all observed areas is correct. At present these data have some narrow residual atmospheric and stellar spectral features which will be removed as the calibrations are refined.

Figure 1 shows a range of spectral and albedo types observed for a number of regions on Mars. As expected, the steep visible slope is relatively smooth, in contrast to ferric-oxide minerals with long-range crystalline structure. However, definite slope changes are visible near 0.53$\mu$m and 0.63$\mu$m, related to incipient ferric-iron crystal-field absorptions. These features indicate a slightly greater degree of crystallinity for the common weathered soil on Mars than seen for the least-crystalline Hawaiian palagonites. The low-albedo region Margaritifer Sinus has a well-developed $Fe^{2+}$ band with a minimum near 0.95$\mu$m, indicating low-Ca, high-Fe clinopyroxene [2]. Slightly different pyroxene band depth and position are seen for Meridiani Sinus in Figure 4. Spectral differences related to $Fe^{3+}$ mineralogy and/or crystallinity are seen in the other figures. The Acidalium spectrum in Figure 2 is less absorbing in the visible than a typical dark region (Margaritifer) but more highly absorbing at longer wavelengths. We interpret these spectral differences as indicating a somewhat more-crystalline ferric oxide at this location on the planet [e.g. 3]. In Figure 3 spectra for Margaritifer Sinus and a region at the southern extreme of Acidalium overlay very well except at wavelengths between roughly 0.8 and 0.9$\mu$m. Such a difference is best explained by variation in a *different* $Fe^{3+}$ crystal-field absorption as seen in the previous example.

These new results, as well as those of others [4], are refining our knowledge of Mars surface composition on a local to regional scale. Greater variation has been observed, related to differing compositions and processes. It should be noted, however, that most of the spectral differences we have seen so far are relatively subtle. Typical high-albedo regions such as Arabia still indicate limited long-range $Fe^{3+}$ crystalline structure in the common weathered soils and dust.

[1] Hapke, B. (1981) **JGR, 86**, 3039.
[2] Adams, J.B. (1974) **JGR, 79**, 4329.
[3] Singer, R.B. (1982) **JGR, 87**, 10159; Sherman, D. *et al.* (1982) **JGR, 87**, 10169.
[4] Bell, J.F. III *et al.* (1990) **JGR**, in press.

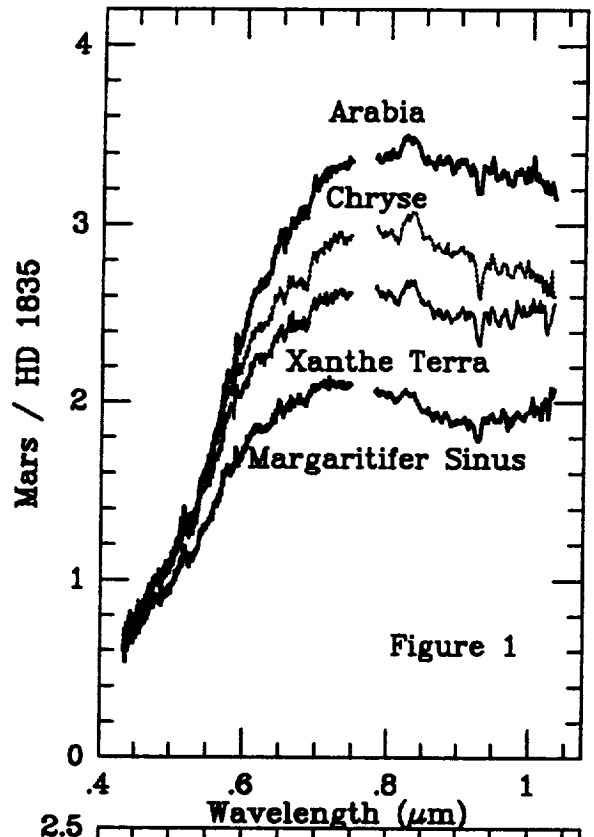


Figure 1

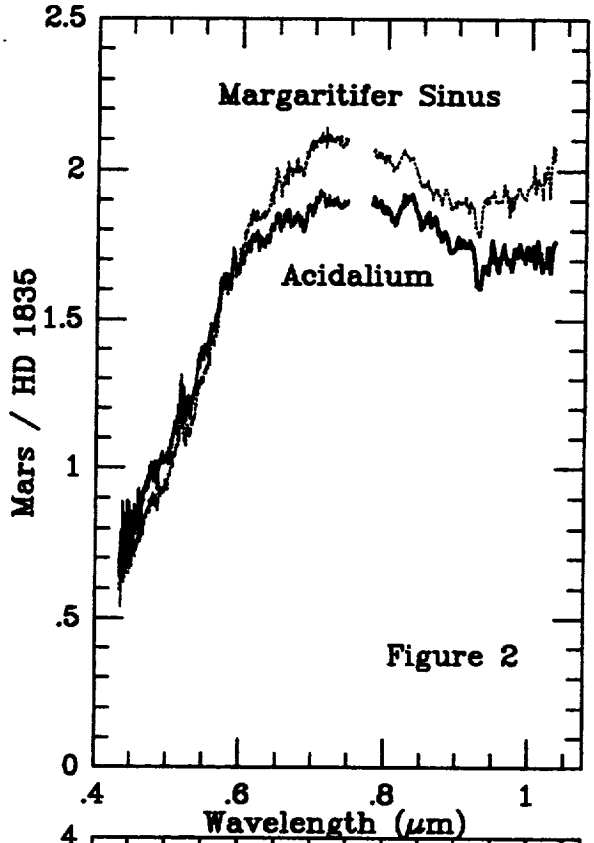


Figure 2

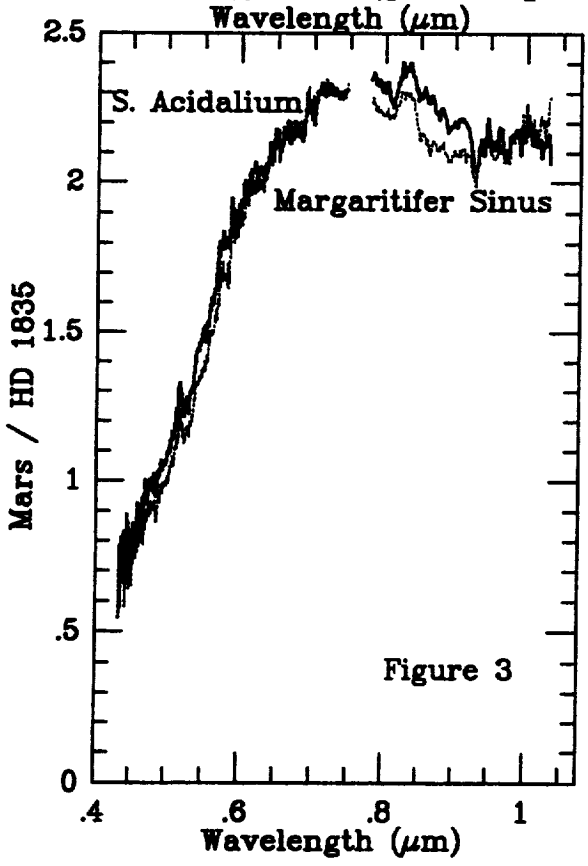


Figure 3

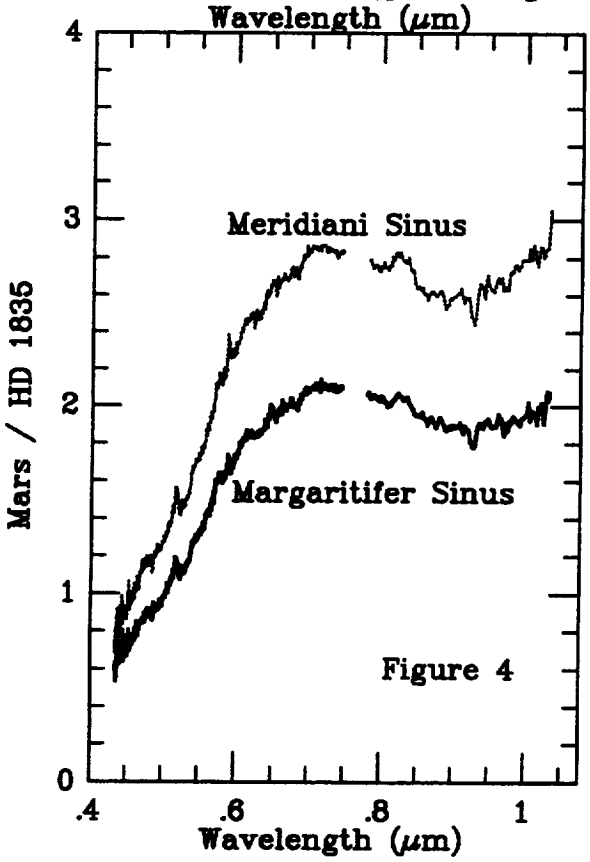


Figure 4

DRY CARBONATE FORMATION ON MARS: A PLAUSIBLE SINK FOR AN EARLY DENSE $CO_2$ ATMOSPHERE? Stuart K. Stephens and David J. Stevenson, Division of Geological and Planetary Sciences, California Institute of Technology, Pasadena, CA 91125.

The Problem. Morphological features on the present surface of Mars suggest to many observers [1-5] that Mars once had an atmosphere with a pressure greater than the ~1 bar thought to be required for an atmospheric greenhouse. Pollack et al. (1987) [4], among others, have discussed models of carbonate formation and recycling to buffer the early $CO_2$ pressure in such an atmosphere. However, since carbonate formation is usually assumed to require standing liquid water at the surface, there is a problem with such carbonate cycles, in that the transition from a greenhouse atmosphere to a pressure of a few millibars (too cold for liquid water) would seem to require an additional mechanism for reducing the atmospheric pressure.

Alternative sinks for the early atmosphere (to bring the pressure below ~1 bar) include impact erosion of the atmosphere [6] and adsorption in the regolith [7]. However, impact erosion would have been most important before the end of the late heavy bombardment (3.8 Gyr); thus, its dominant effect may have preceded a greenhouse atmosphere which lasted until later. Also, adsorption in the regolith is thought to be only marginally capable of storing 1 bar of $CO_2$, and this is a sink that would necessarily have been filled -- and therefore unavailable for further use -- during the time of greenhouse conditions.

This work investigates another alternative sink for an early dense $CO_2$ atmosphere on Mars: dry carbonate formation.

Booth and Kieffer's Experiment. An experiment performed by Booth and Kieffer (1978) [8] seemed to demonstrate that carbonate will form on silicate grains under Martian conditions in the absence of liquid water. Their result was $10^{12-13}$ molecules of carbonate evolved per $cm^3$ per second -- yielding much less than a monolayer of carbonate on ~40 μm grains in the span of several days. The authors show that this reaction rate more than accounts (by several orders of magnitude) for a $CO_2$ inventory of 1 bar over geologic time. However, their study had a major limitation, namely that there is no reliable basis for extrapolation, since less than a monolayer was formed, and the nature of the "rind" formed was not closely examined.

We attempted to find published results where the carbonate formed by $CO_2$ interaction with silicates in the absence of water was actually examined (e.g., with a scanning electron microscope), but without success. Unfortunately, a precise theoretical approach holds little promise either, since the exact nature of any rind formed on a substrate of uncertain character (glass vs. crystals? mono- vs. polyminerallic?) is poorly constrained a priori.

Present Theoretical Work. In the absence of experimental results, then, we considered the worst case -- that in which the formation of a rind limits the effectiveness of the rapid reaction reported by Booth and Kieffer. Namely, we considered the question: Is the process (of dry carbonate formation) reaction-limited or diffusion-limited? This involves comparing: (1) the thickness of the reaction layer formed, assuming infinite diffusivity, with (2) the thickness of the product layer formed (which is a multiple of the diffusion distance $(Dt)^{1/2}$ -- see 2 paragraphs below), assuming infinite reactivity. The result is that the diffusion-limited case requires the diffusivity D to be $< 10^{-9}$ $cm^2$ $s^{-1}$.

Next, the diffusivity of $CO_2$ through carbonate was required. Again, no directly pertinent experimental reports were found in the literature, so we used results of Bhatia and Perlmutter (1983) [9] for diffusion of $CO_2$ through

carbonate formed on lime (CaO). Their experiments were performed at high temperature (> 600 K) and must be extrapolated (using an Arrhenius relation) to low temperature, but this probably results in a conservative (i.e., low) estimate of the diffusivity since diffusion mechanisms other than the one fitted by their data probably operate in the low-temperature regime (i.e., mechanisms with smaller activation energies, thus giving higher diffusivities upon extrapolation). The extrapolated diffusivity is $D \sim 10^{-27}$ $cm^2$ $s^{-1}$, implying a diffusion-limited reaction.

The amount of carbonate formed in such a diffusion-limited case is determined by consideration of tarnishing reactions [10,11], for which the thickness of product formed on a solid by a gas reacting with it is given by a relation involving the densities of gas ($CO_2$) and product (carbonate) -- it reduces to $\ell(t) \sim 0.06\ (Dt)^{1/2}$.

Results. Over geologic time, this diffusion-limited dry carbonate formation is capable of forming a layer ~60 Å thick on silicate grains. For a 1 km regolith and 40 μm particles, this means that ~0.05 bar $CO_2$ can be stored. This is a conservative estimate, since: (1) D is probably higher, and (2) we've assumed that the rind is non-porous. Note, however, that our estimate of the diffusivity places us eighteen orders of magnitude on the diffusion-limited side of the inequality. Even if this estimate is wrong by many orders of magnitude, it implies that the Booth and Kieffer results are irrelevant, because we are in the diffusion-limited regime.

Discussion. The possibility that a significant amount of $CO_2$ can be stored by dry carbonate formation on early Mars has implications for the evolution of atmospheric $CO_2$ pressure after bodies of liquid water were no longer available for aqueous carbonate formation. However, whether the $CO_2$ pressure would have declined gradually or very quickly depends on the precise behavior of the diffusivity, which is a function of temperature and therefore time. The answer awaits further work.

Note that if the carbonate is indeed produced in thin (<< μm) layers, as described above, then it may not be readily observable by current remote sensing techniques. Thus, the proposed $CO_2$ storage mechanism cannot be said to be inconsistent with the latest near-infrared telescopic observations [12] which do not reliably detect carbonate.

Conclusions. Thus, we have used assumptions concerning the validity of published experimental work, and conservative estimates of parameters and mechanisms, to arrive at the result: Dry carbonate formation is almost certainly diffusion-limited and the results of Booth and Kieffer are irrelevant. Even with a very low diffusivity, the tarnishing process may provide a significant sink for atmospheric $CO_2$ on early Mars. It may therefore help explain the transition from an early dense atmosphere to the present low pressure.

References. [1] J.C. Walker (1978). In Comparative Planetology, C. Ponnamperuma, ed. Academic Press, New York. [2] J.B. Pollack (1979), Icarus, 37, 479-553. [3] R. Kahn (1985), Icarus, 62, 175-190. [4] J.B. Pollack et al. (1987), Icarus, 71, 203-224. [5] C.P. McKay and C.R. Stoker (1989), Rev. Geophys., 27(2), 189-214. [6] H.J. Melosh and A.M. Vickery (1989), Nature, 338, 487-489. [7] F.P. Fanale et al. (1982), Icarus, 50, 381-407. [8] M.C. Booth and H.H. Kieffer (1978), J. Geophys. Res., 83, 1809-1815. [9] S.K. Bhatia and D.D. Perlmutter (1983), AIChE J., 29(1), 79-86. [10] F. Booth (1948), Trans. Faraday Soc., 44, 796-801. [11] J. Crank (1956). The Mathematics of Diffusion. Clarendon Press, Oxford. [12] D.L. Blaney and T.B. McCord (1989), J. Geophys. Res., 94, 10159-10166.

WHY EXISTING TERRESTRIAL PLANET THERMAL HISTORY CALCULATIONS SHOULD NOT BE BELIEVED (AND WHAT TO DO ABOUT IT); David J. Stevenson and Seth S. Bittker, 170–25, Caltech, Pasadena, CA 91125.

*Introduction.* Beginning in the late 1970's, many workers have used simple parameterized convection recipes for analyzing the thermal history of a terrestrial planet [1–3]. These calculations assume that thermally derived density differences are the only important contribution to convective instability. However, all planets undergo irreversible differentiation and the resulting density effects are locally far larger than thermal effects. This is not a novel observation, but the past response has usually been that the total gravitational energy release which accompanies irreversible differentiation is smaller than that associated with thermal convection and hence energetically less important. Although the latter statement is true (excluding core formation which is believed to be completed very early in all cases [4]), it does not get to the heart of the issue, which is this: This correct parameterization of convection requires a *boundary layer* analysis and it is precisely in this layer where compositional effects can be large because of partial melting. Since the residue left from partial melting is generally less dense than the undepleted mantle below (mainly because the melt is relatively Fe-rich), volcanism can *stabilize* the convective system and even shut the convection off, at least temporarily. This is an especially serious effect on one-plate planets because the lithosphere is not fully participating in the return flow.

*Background and Input.* Compositional effects associated with basaltic production play a role in the subductability of the Earth's oceanic lithosphere [5], the dynamics of matrix flow and melt migration beneath mid-ocean ridges [6] and in the mantle wedge above subduction zones [7], and in the global contraction or expansion of a planet [8]. We can identify the following regimes of interest:

I. The convective temperature profile (conductive lid and adiabatic interior) never intercepts the mantle solidus. Conventional parameterized recipes will then apply; however, this is an uninteresting case, even in smaller planets, since one plate planets usually "run hot" (because one plate planets are less efficient in eliminating heat) and do not lie in this regime, except when all the basaltic component has been flushed out.

II. Adiabat extends into the supersolidus region, though only to a small extent and not so as to deplete all basalt from the material in that region. Here, we can modify the "local" Rayleigh number and devise the following computational scheme, analogous to those used in the past for purely thermal buoyancy (e.g., ref. 3). We set $F = k\Delta T/\delta$, $Ra \equiv g(\alpha\Delta T - \beta f)\delta^3/\nu(T - \Delta T/2)\kappa$, $d(Ra)/d\delta = 0$, and $Ra = 10^3$ at this extremum. Parameters have their usual meanings (F = heat flow, k = thermal conductivity, g = gravity, $\alpha$ = coefficient of thermal expansion, $\delta$ = boundary layer thickness, $\nu$ = temperature-dependent viscosity, $\kappa$ = thermal diffusivity, $\Delta T$ = temperature drop across the boundary layer) and the crucial change is the $\beta f$ term representing the density effect arising from a degree of melting f, averaged within the boundary layer. The value of $\beta$ is a material property that will vary among planets (see below), and allowance must also be made for the *fertility*: the extent to which the mantle still has the "primordial" basaltic (i.e., pyroxene-rich) component.

III. Large excursion of the adiabat into the supersolidus region. In this case, a secondary convection pattern can initiate within the zone of partial melting since all of this zone is denuded of basalt but has an unstable temperature gradient. This convection will *not* penetrate into the deeper mantle, which is intrinsically more dense (more iron-rich). The analysis so far has, however, ignored phase boundaries which will surely complicate these considerations.

*Applications.* We have done a detailed analysis of regime II, and made some analysis of the implications for Mars. In the Figure, we show total heat flux vs. mantle temperature for a variety of values of $\beta$. (Ignore the flat curve at $T < 1600$ K which corresponds to pure conduction.) The smooth upward curvature at small $\beta$ corresponds to the usual expectation

that heat flow increases dramatically with increasing "mantle temperature" (here defined as the zero pressure extrapolation of the mantle adiabat). But at sufficiently large $\beta$ ($\geq$0.04), we find a turnover in the curves, reflecting the increasing stabilization of convection. What is a reasonable value for $\beta$? On Mars, where most estimates of mantle iron content are high, the implication of the work of Finnerty *et al.* [9], for example, is $\beta \approx 0.1$, very large and easily enough to have an *enormous* effect on the convection. The result is that the mantle heats up, enters regime III, and begins to form convective *layers*. The value of $\beta$ on Earth, Venus, and possibly Mercury is smaller by a factor of about 2, but still big enough to be very important. (Remember, however, that the model is not meant to apply to Earth.)

*Implications.* Although detailed models of the resulting thermal evolution have not been completed (they are much harder than previous simple models), it is clear that they will be markedly different from previous work. Here are the main differences: (1) A tendency for the interior to *heat up* at depth even in early history, because volcanism stifles convection. This is in contrast to the trend toward monotonic cooling models and volcanism histories [e.g., 10]. (2) A tendency for episodes of volcanism, separated by long periods of time associated with the merging of convecting layers operating in regime III. (3) Delayed heat loss and the likelihood of continued volcanism on Mars.

## References

1. Schubert, G., Cassen, P., and Young, R.E. (1979). *Icarus* **38**, 192.
2. Stevenson, D.J., Spohn, T., and Schubert, G. (1983). *Icarus* **54**, 466.
3. Solomatov, V.S., Leontjev, V.V., and Zharkov, V.N. (1987). *Gerlands Beitr. Geophysik* **96**, 73.
4. Stevenson, D.J. (1990). In *Origin of the Earth*, in press.
5. Oxburgh, E.R. and Parmentier, E.M. (1977). *J. Geol. Soc. London* **133**, 343.
6. Scott, D.R. and Stevenson, D.J. (1989). *J. Geophys. Res.* **94**, 2973.
7. Davies, J.H. and Stevenson, D.J. (1990). *J. Geophys. Res.*, submitted.
8. Kirk, R.L. and Stevenson, D.J. (1989). *J. Geophys. Res.* **94**, 12,133.
9. Finnerty, A.A., Phillips, R.J., and Banerdt, W.B. (1988). *J. Geophys. Res.* **93**, 10,225.
10. Schubert, G. *et al.* (1990). In *Mars*, Univ. Arizona Press, in press.

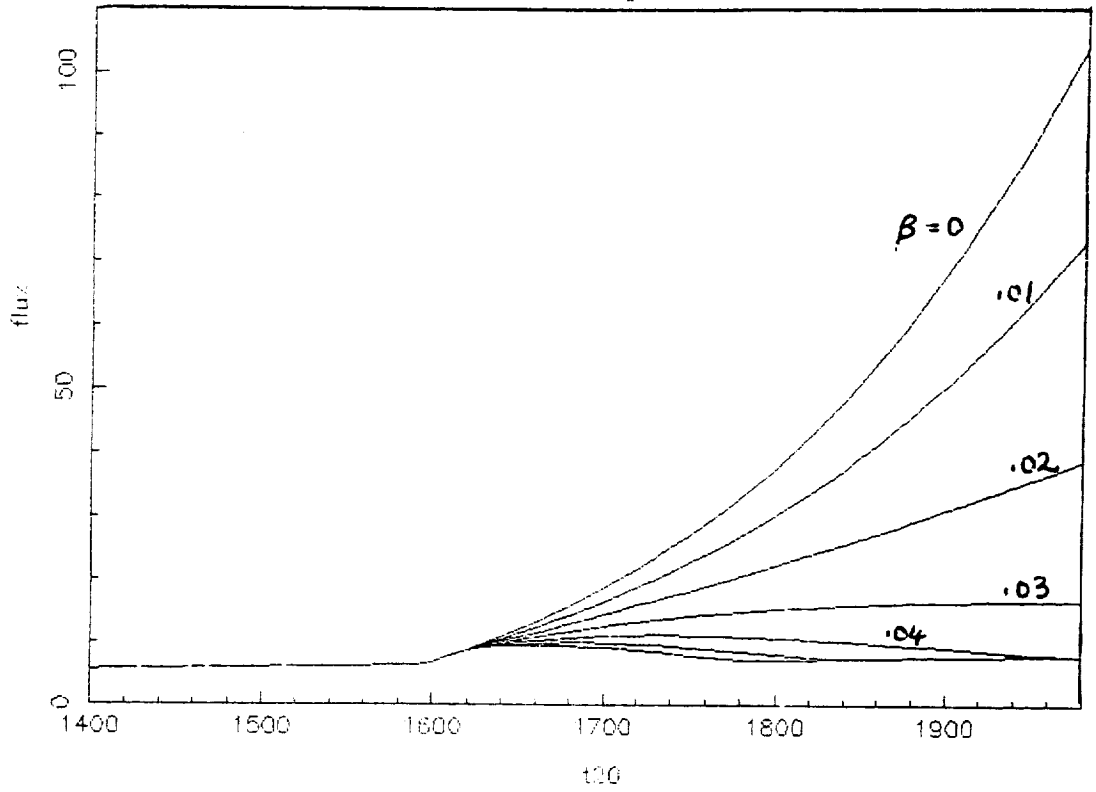

# FERROLYSIS OF IRON-BEARING MARTIAN BRINES: ORIGIN OF DUST-STORM PARTICULATES ON MARS

**D'Arcy W. Straub and Roger G. Burns**, Department of Earth, Atmospheric and Planetary Sciences, Massachusetts Institute of Technology, Cambridge, Massachusetts 02139.

**INTRODUCTION.** Brines have been proposed on Mars [1] to explain salt weathering erosional features [2], regions of high radar reflectivity [3,4], and the high concentrations of S and Cl in Viking Lander XRF measurements of the regolith [5]. These elements were interpreted to be present as chlorides and sulfates in evaporites [6] and gossans [7]. The formation of such evaporite and gossaniferous deposits implies that oxidative weathering reactions in an aqueous environment must have occurred sometime during the evolution of the martian surface. However, such water environments are not conspicuous on the surface of Mars now, except perhaps in the Solis Lacus region (14°-22°S; 84°-120°W) and other areas of comparable latitudes [8] having high radar reflectivities [3] from which local and global dust storms appear to originate [9,10]. Attention on possible martian brine compositions has focussed on eutectic temperatures of salt mixtures containing chlorides and sulfates of Na, K, Mg and Ca [1,4]. However, other dissolved cations must also be present in such brines, particularly ferric and ferrous iron, which are stabilized in aqueous solutions at relatively low values of pH (acidity) and Eh (redox potential) [7].

Ferrolysis, the process of oxidation of ferrous iron accompanied by the hydrolysis of ferric iron, is the ultimate fate of dissolved iron and is likely to occur during sublimation and melting of the permafrost on Mars [11], leading to the precipitation of iron phases which could be transported around the planet in dust storms. This has led to a study of residues formed during the oxidation and precipitation of iron phases from evaporated salt solutions. We report here preliminary results on the nature of ferrolysis products that might have been deposited from martian brines and be constituents of dust storms on Mars.

**EXPERIMENTAL PROCEDURES.** A number of mixed-salt solutions were prepared from sulfates and chlorides of Mg, K, and Na, to which were added ferrous sulfate. During the experiment, air was bubbled through the solutions to increase the rate of oxidation. In some cases, solutions were acidfied to stabilize ferric iron, or the pH was adjusted to produce a precipitate. Other solutions were allowed to evaporate at ambient temperatures. Precipitates from the solutions and products of evaporation were examined by Mossbauer spectroscopy to determine the formation of ferric iron and to identify the ferric hydrolysates. Measurements made at liquid helium temperature (4.2K) proved to be particularly useful for characterizing the nanophase precipitates.

**RESULTS.** For nearly every experiment performed, regardless of length, akaganéite (β-FeOOH) was at least one of the observed ferrolysis products. These results seem to violate formerly observed trends concerning ferric hydrolysis products. For brine compositions containing $SO_4$, goethite (α-FeOOH) or hematite (α-$Fe_2O_3$), depending upon the $SO_4$ / Fe ratio, are the expected hydrolysis products [12]. Generally, β-FeOOH is expected in solutions where Cl or F is present [13]. In the presence of Na and K, jarosite [(K,Na)$Fe_3(SO_4)_2(OH)_6$] is another potential hydrolysis product [14].

Acidified solutions, where the $Fe^{3+}$ ion is stabilized, produced complex ferrolysis reactions when evaporation neared completion. Mossbauer spectra at 4.2K of several samples exhibited two magnetic sextets. In the case where Na was present in the brine, magnetic sextets correponding to β-FeOOH and jarosite were observed. Only one magnetic sextet, corresponding to β-FeOOH, was observed when K was present in the brine though.

The experiments performed to present indicate that in high ionic strength solutions, representative of the brines on Mars, the ferrolysis products on Mars may not be easily inferred. First, β-FeOOH appeared in most reactions, regardless of the compostion of the brine solution. Second, under the influence of evaporation, jarosite often appeared. Further studies are needed, however, to

determine if β-FeOOH is always a product in high ionic strength solutions and to better characterize the conditions under which jarosite is formed when evaporation occurs.

**ORIGIN OF DUST STORM PARTICULATES.** Experimental measurements described in an accompanying abstract [15] and geochemical models published elsewhere [7,11,16] suggest that acid weathering has been a significant surface process on Mars and that groundwater, now permafrost, may be acidic. Such low pH solutions dissolve significant concentrations of silica, Al, Mg, Fe, and other ionic species. They also hold in suspension considerable amounts of monodispersed sols of hydrous oxides and sulfates of Fe and Al [11]. These ions and sols are precursors to clay silicate, oxyhydroxide and hydroxo sulfate minerals which form as precipitates in response to changes of temperature, pH and salinity.

On the surface of Mars, volatilization of $H_2O$ during sublimation of permafrost or evaporation of the brine eutectic will induce the precipitation of dissolved salts of Na, Ca, Mg, $Fe^{2+}$, etc. and cause the flocculation of colloidal ferric-bearing aluminosilicate, oxide, oxyhydroxide and hydroxo sulfate phases. These nanophase materials may constitute the particulates of local and global dust storms when they are generated in the Solis Lacus and similar regions of low radar reflectivities on Mars. During aeolian transport, any unoxidized ferrous salts liberated from volatilized permafrost will be completely oxidized, while dessication of ferric hydrolysis products to $Fe_2O_3$ phases [17] will be facilitated. Such ferric oxides include the formation of maghemite from lepidocrocite [18] considered to be the magnetic phase on Mars [19], as well as the occurrence of nanophase hematite believed to be present in bright regions of Mars [20].

**REFERENCES.** [1] G.W.Brass, *Icarus*, 42, 20 (1980); [2] M.C.Malin, *JGR*, 79, 3888 (1974); [3] S.H.Zisk & P.J.Mouginis-Mark, *Nature*, 44, 735 (1980); [4] A.P.Zent & F.P.Fanale, *JGR*, 91, D439 (1986); [5] P. Toulmin *et al.*, *JGR*, 82, 4625 (1977); [6] B.C.Clark & D.C.Van Hart, *Icarus*, 45, 370 (1981); [7] R.G.Burns, *Proc. 18th LPSC*, 713 (1988); [8] L.E.Roth *et al.*, *Lunar Planet.Sci.*, XVI, 712 (1987); [9] G. De Mottoni, *Icarus*, 25, 296 (1975); [10] S.W.Lee, *Lunar Planet.Sci.*, XVI. 483 (1987); [11] R.G.Burns, *Proc. 17th LPSC, JGR*, 92, E570 (1987); [12] J. Dousma *et al.*, *J. Inorg. Nucl. Chem.*, 41, 1565 (1979); [13] M. Ohyabu and Y. Ujihira, *J. Inorg. Nucl. Chem.*, 43, 3125 (1981); [14] J. Dutrizac and S. Kaiman, *Can. Mineral.*, 14, 151 (1976); [15] R.G.Burns & D.S.Fisher, *Lunar Planet. Sci.*, XXI, 145 (1990); [16] R.G.Burns & D.S.Fisher, *LPI Tech. Rept.*, 88-05, 34 (1988);*JGR*, in press; [17] J.L.Gooding, *Icarus*, 33, 483 (1978); [18] J.Posey-Dowty *et al.*, *Icarus*, 66, 105 (1986); [19] R.B.Hargraves *et al.*, *JGR*, 82, 4547 (1977); [20] R.V.Morris *et al.*, *JGR*, 94, 2760 (1989); [21] Research supported by NASA grants NSG-7604 and NAGW-1078.

# OXIDIZED PYROXENES AND DEGRADATION OF THEIR VISIBLE - NEAR INFRARED SPECTRA: IMPLICATIONS TO REMOTE-SENSING OF MARS

**D'Arcy W. Straub and Roger G. Burns**, Department of Earth, Atmospheric and Planetary Sciences, Massachusetts Institute of Technology, Cambridge, Massachusetts 02139.

**INTRODUCTION.** Pyroxenes and olivines in basaltic magma extruding onto surfaces of terrestrial planets such as Mars, Earth and Venus are vulnerable to atmospheric oxidation during cooling of the igneous rocks. Ferrous iron in these ferromagnesian silicates may be oxidized to structural $Fe^{3+}$ ions or form a veneer of ferric oxide phases that might obliterate the diagnostic $Fe^{2+}$ crystal field (CF) spectral features used to identify pyroxenes and olivines. Previous measurements of oxidized olivines [1] demonstrated that the appearance of $Fe_2O_3$ phases (hematite, maghemite) obscure the characteristic olivine bands at 0.85, 1.05 and 1.20 μm. The 1 micron and 2 micron regions used to identify pyroxene structure-types and compositions in telescopic spectral measurements [2,3] may be similarly compromised. We report here measurements made on heated pyroxenes to assess the effects of aerial oxidation on their visible-near infrared spectra.

**PYROXENE SPECIMENS.** A suite of well-characterized pyroxenes [4] representative of different structure-types and compositions was chosen for the spectroscopic measurements and consisted of orthopyroxene, $Fe_{29}Mg_{70}Ca_1$; pigeonite, $Fe_{37}Mg_{47}Ca_{16}$; augite, $Fe_{10}Mg_{41}Ca_{46}$; a hedenbergite, $Fe_{42.5}Mg_{10}Ca_{47.5}$ containing 10% $Fe^{3+}$ [5]; and a Mn hedenbergite, $Fe_{40}Mn_{10}Mg_{0.5}Ca_{49.5}$. The specimens were selected to encompass different site occupancies of iron cations in the pyroxene crystal structure, particularly the M2 position, since $Fe^{2+}$ ions in this highly distorted non-centrosymmetric site are responsible for the positions and intensities of the diagnostic pyroxene "1 micron" and "2 micron" absorption bands [3]. Ferrous ions located in less distorted pyroxene M1 sites contribute relatively weak absorption bands centered near 0.9 and 1.15 μm [3,6,7]. In magnesian orthopyroxenes and pigeonites, the $Fe^{2+}$ ions are strongly enriched in the M2 positions with relatively small proportions in the M1 positions [8]. In calcic clinopyroxenes, although the $Fe^{2+}$ ions are more concentrated in the M1 positions, they preferentially fill any $Ca^{2+}$ vacancies in the M2 positions except in competition with $Mn^{2+}$ ions, which have a stronger preference than $Fe^{2+}$ for the pyroxene M2 positions [8]. The Mn hedenbergite, therefore, was expected to contain negligible $Fe^{2+}$ ions in its M2-sites.

**EXPERIMENTAL DETAILS.** Powdered pyroxenes (particle sizes <45 microns) were heated in air in the temperature range 400-800°C for different time periods. Mossbauer spectra at ambient temperatures and at 4.2K were used to identify the appearance of ferric iron in the oxidized pyroxenes. For most specimens, only ferric doublets (in addition to ferrous doublets) were present in the 295K Mossbauer spectra, but at 4.2K sextets attributable to ferric oxides (hematite, maghemite or magnesioferrite) were weakly developed indicating the formation of nanophase $Fe_2O_3$ phases in and on the surfaces of the pyroxene crystallites. The 4.2K spectra also indicated magnetic ordering of structural $Fe^{2+}$ and $Fe^{3+}$ ions in the two hedenbergites. Visible - near infrared reflectance spectra of selected samples were measured by Steve Pratt at Brown University using the RELAB facility there [9].

**RESULTS.** Examples of reflectance spectra of different pyroxenes oxidized in air are illustrated in Figures 1 to 4. Two extreme situations reflecting different $Fe^{2+}$ site occupancies are demonstrated by the spectra of orthopyroxene (Fig.1) and Mn-hedenbergite (Fig.4). In orthopyroxene, M2-site $Fe^{2+}$ ions are responsible for the absorption bands at 0.9 and 1.8 μm, the band depths of which are considerably reduced by oxidation of $Fe^{2+}$ to $Fe^{3+}$ ions. After heating in air, the increased absorption between 0.4 and 0.9 μm may be attributed to $Fe^{3+}$ CF transitions (which, for hematite, occur at 0.44, 0.51, 0.65 and 0.88 μm [10]) and to $Fe^{2+} \rightarrow Fe^{3+}$ intervalence charge transfer transitions (IVCT) occurring in orthopyroxene around 0.7 μm [6]. The Mn-hedenbergite spectra (Fig.4) originating from CF transitions in M1-site $Fe^{2+}$ at approx. 0.95 and 1.15 μm are severely modified after oxidation by spectral features attributable to nanophase $Fe_2O_3$ and structural $Fe^{3+}$, particularly the $Fe^{2+} \rightarrow Fe^{3+}$ IVCT occurring in calcic clinopyroxenes around 0.8 μm [5,6]. In the spectrum of the $Ca^{2+}$-deficient hedenbergite (Fig. 3), the M2-site $Fe^{2+}$ CF bands at 1.05 and 2.3 μm are obliterated by oxidation of $Fe^{2+}$ to $Fe^{3+}$, a similar trend also being observed in the spectra of the heated augite (Fig. 2).

**DISCUSSION.** The reduced band depths of the pyroxene 1 micron and 2 micron spectral features may be attributed to two related causes: first, loss of $Fe^{2+}$ ions in the pyroxene M2 sites after they become oxidized to $Fe^{3+}$ ions; and second, increased absorption by the ferric iron, either as structural $Fe^{3+}$ ions in the pyroxenes, or as nanophase $Fe_2O_3$ formed in and on the surfaces of the pyroxene grains. Similar contrasts of band depths may be seen between dark-region and bright-region spectra of Mars [11]. These and earlier results [1] suggest a mechanism for producing the nanophase hematite popularly considered to be responsible for the features observed around 0.65 and 0.87 μm in remote-sensed reflectance spectral profiles of Mars [12,13]: it results from aerial oxidation of structural $Fe^{2+}$ ions in olivines and pyroxenes to highly disseminated $Fe_2O_3$ [14].

**REFERENCES.** [1] K.S.Bartels & R.G.Burns, *Lunar Planet. Sci.*, XX, 44 (1989); [2] J.B.Adams, *JGR*, 79, 4829 (1974); [3] R.G.Burns, *Min. Mag.*, 53, 135 (1989); [4] M.D.Osborne *et al.*, *Proc. 9th LPSC*, 2949 (1978); [5] R.G.Burns & F.E.Huggins, *Am. Min.*, 58, 955 (19730; [6] G.R.Rossman, *Rev. Min.*, 7, 93 (1980); [7] G.Steffen *et al.*, *Phys. Chem. Min.*, 16, 120 (1988); [8] M.Cameron & J.J.Papike, *Rev. Min.*, 7, 5 (1980); [9] C.Pieters, *JGR*, 90, 12393 (1985); [10] D.M.Sherman & T.D.Waite, *Am. Min.*, 70, 1262 (1985); [11] R.B.Singer, *Adv. Space Sci.*, 5, 59 (1985); [12] R.V.Morris *et al.*, *JGR*, 94, 2760 (1960); [13] J.P.Bell *et al.*, *JGR*, in press; [14] Research supported by NASA grants NGR 7604 and NAGW 1078. We thank Steve Pratt for the reflectance spectral measurements.

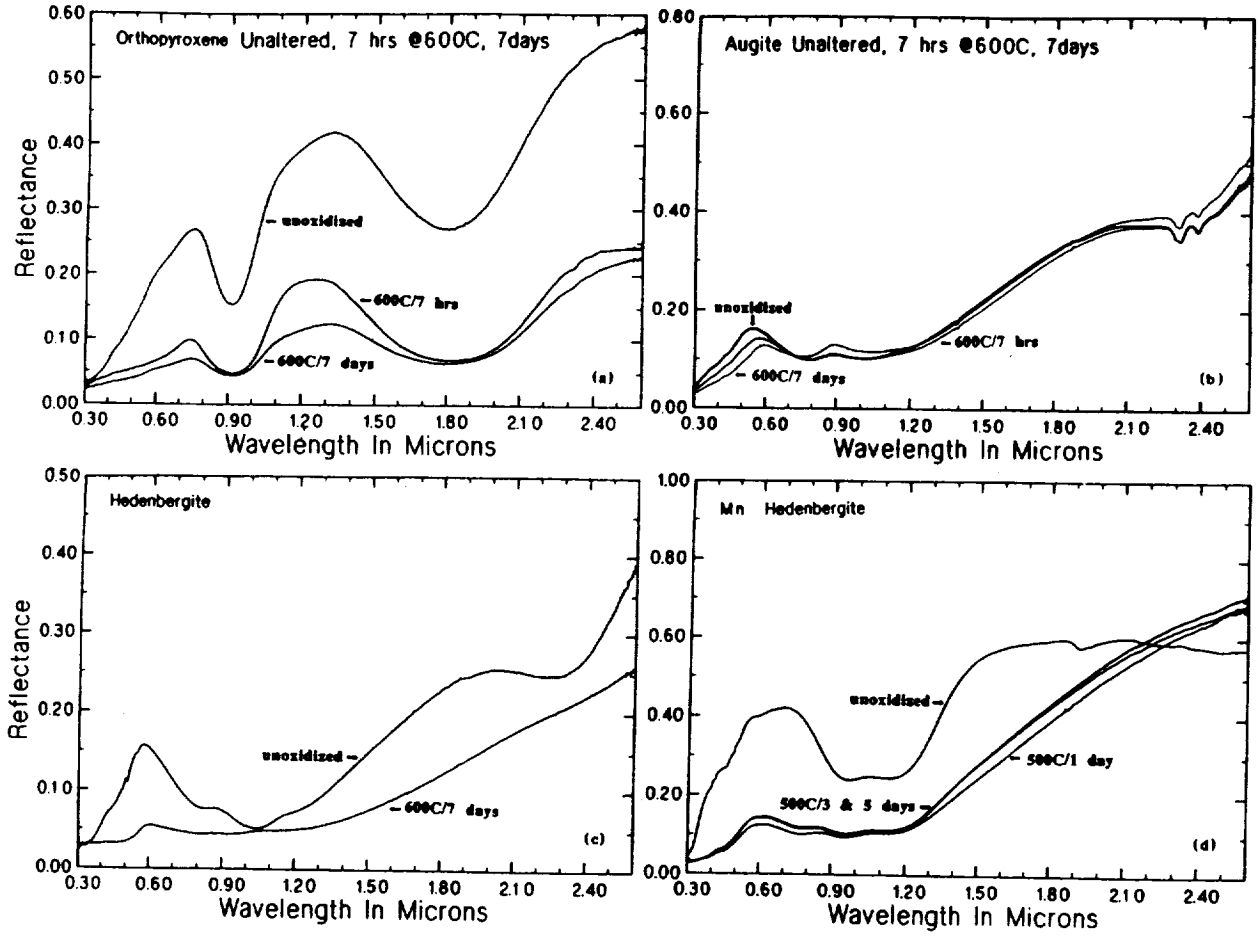


**FIGURE 1.** Reflectance spectra of pyroxenes before and after aerial oxidation. (a) orthopyroxene; (b) augite; (c) hedenbergite; and (d) Mn hedenbergite.